Interaction between the T4 Helicase Loading Protein (gp59) and the DNA Polymerase (gp43): Unlocking of the gp59–gp43–DNA Complex to Initiate Assembly of A Fully Functional Replisom...

ARTICLE *in* BIOCHEMISTRY · JUNE 2005

Impact Factor: 3.02 · DOI: 10.1021/bi047296w · Source: PubMed

7 AUTHORS, INCLUDING:

Jun Xi
Drexel University
27 PUBLICATIONS **563** CITATIONS
SEE PROFILE

Zhiquan Zhang
Nantong University
28 PUBLICATIONS **465** CITATIONS
SEE PROFILE

Zhihao Zhuang
University of Delaware
49 PUBLICATIONS **1,052** CITATIONS
SEE PROFILE

Jingsong Yang
GlaxoSmithKline plc.
30 PUBLICATIONS **921** CITATIONS
SEE PROFILE

Interaction between the T4 Helicase Loading Protein (gp59) and the DNA Polymerase (gp43): Unlocking of the gp59−gp43−DNA Complex to Initiate Assembly of A Fully Functional Replisome†

Jun Xi,[⊥,§] Zhiquan Zhang,[‡,§] Zhihao Zhuang,[⊥] Jingsong Yang,[⊥] Michelle M. Spiering,[⊥] Gordon G. Hammes,[‡] and Stephen J. Benkovic*[,⊥]

Department of Chemistry, Pennsylvania State University, 104 Chemistry Building, University Park, Pennsylvania 16802, and Department of Biochemistry, Duke University Medical Center, Box 3711, Durham, North Carolina 27710

Received December 23, 2004; Revised Manuscript Received February 9, 2005

ABSTRACT: Single-molecule fluorescence resonance energy transfer and functional assays have been used to study the initiation and regulation of the bacteriophage T4 DNA replication system. Previous work has demonstrated that a complex of the helicase loading protein (gp59) and the DNA polymerase (gp43) on forked DNA totally inhibits the polymerase and exonuclease activities of gp43 by a molecular locking mechanism (Xi, J., Zhuang, Z., Zhang, Z., Selzer, T., Spiering, M. M., Hammes, G. G., and Benkovic, S. J. (2005) *Biochemistry 44*, 2305−2318). We now show that this complex is "unlocked" by the addition of the helicase (gp41) with restoration of the DNA polymerase activity. Gp59 retains its ability to load the helicase while forming a gp59−gp43 complex at a DNA fork in the presence of the single-stranded DNA binding protein (gp32). Upon the addition of gp41 and MgATP, gp59 dissociates from the complex, and the DNA-bound gp41 is capable of recruiting the primase (gp61) to form a functional primosome and, subsequently, a fully active replisome. Functional assays of leading- and lagging-strand synthesis on an active replication fork show that the absence of gp59 has no effect on the coupling of leading- and lagging-strand synthesis or on the size of the Okazaki DNA fragments. We conclude that gp59 acts in a manner similar to the clamp loader to ensure proper assembly of the replisome and does not remain as a replisome component during active replication.

The bacteriophage T4 replisome is composed of eight proteins that form distinct units within the replication complex (*2*−*4*). These units are the primosome (a complex of the primase, gp61, bound to the helicase, gp41),[1] the leading- and lagging-strand holoenzymes (each composed of a DNA polymerase, gp43, and a sliding clamp, gp45), and the single-stranded DNA binding protein, gp32. These units are assembled with the assistance of the clamp loader, gp44/62, and helicase loading protein, gp59, to form the replisome that is responsible for highly processive and efficient DNA replication. The primosome and the holoenzymes are assembled individually with the helicase loading protein gp59 largely responsible for coordinating key aspects of assembly and regulation of these three units (*1*, *5*−*7*).

The helicase loading protein gp59 was first discovered as an auxiliary T4 replication protein (*8*) whose function in replisome assembly is to recruit and load the helicase, gp41 (*9*), at a replication fork coated by the single-stranded DNA binding protein, gp32 (*10*). The assembled hexameric gp41 (*11*) moves in the 5′ to 3′ direction on the lagging strand to unwind the double-stranded DNA ahead of the holoenzyme in an ATP or GTP-driven process. Crystallographic studies of gp59 (*12*) have shown that this protein is an almost completely helical protein with a shallow central groove on one surface of the protein between the N- and C-terminal domains. The N-terminal domain of gp59 exhibits a significant structural homology (*12*) to a family of eukaryotic HMG-1 proteins. Like HMG-1 proteins, gp59 prefers to bind branched DNA structures, such as forked DNA with either single-stranded or partially duplex arms (*12*, *13*). Gp59 modulates the binding of gp41 to DNA as well as its ATPase activities (*14*) on both single-stranded DNA and forked DNA by interacting with the C terminus of gp41 (*13*). The steady-state rate of DNA unwinding by gp41 is increased by 200-fold in the presence of gp59 (*15*). Gp59 also stimulates gp41

† This research was supported by grants from the National Institutes of Health, GM65128 (G.G.H.), GM071130 (M.M.S.), and GM13306 (S.J.B.).

* To whom the correspondence should be addressed. Mailing address: The Pennsylvania State University, 414 Wartik Laboratory, University Park, PA 16802. Telephone: (814)865-2882. Fax: (814)-865-2973. E-mail: sjb1@psu.edu.

⊥ Pennsylvania State University.

§ These authors contributed equally to this work.

‡ Duke University Medical Center.

[1] Abbreviations: P−T junction, primer−template junction of duplex DNA.; gp32, single-stranded DNA binding protein; gp41, helicase; gp43, DNA polymerase; gp43(exo-), exonuclease-deficient gp43; gp44/62, clamp loader; gp45, processivity clamp for DNA polymerase; gp59, helicase loading protein; gp61, primase; A488, Alexa Fluor 488; A555, Alexa Fluor 555; FRET, fluorescence resonance energy transfer; Tris, tris(hydroxymethyl)aminomethane; SDS, sodium dodecyl sulfate; DTT, dithiothreitol; EDTA, ethylenediamine tetraacetic acid, disodium salt; dNTPs, deoxyribonucleotide triphosphates; dATP, deoxyadenosine triphosphate; dCTP, deoxycytidine triphosphate; dGTP, deoxyguanosine triphosphate; dTTP, deoxythymidine triphosphate; rNTPs, ribonucleotide triphosphates; ATP, adenosine triphosphate; ATPγS, adenosine 5′-*O*-3-thiotriphosphate; GTP, guanosine triphosphate; CTP, cytidine triphosphate; UTP, uridine triphosphate; PAGE, polyacrylamide gel electrophoresis.

10.1021/bi047296w CCC: $30.25
Published on Web 05/05/2005

helicase activity on four-way junctions and on DNA substrates that mimic a D-loop structure (*13*). The maximum activity of DNA unwinding occurs when gp59 and gp41 are in a 1:1 stoichiometry (*15*). Since chemical cross-linking studies (*16*) suggest that gp59 can induce the oligomerization of gp41 to form a hexameric ring, it is probable that gp59 may also form a hexameric ring structure while bound to the forked DNA, even though no rigorous studies to date have been done to establish the nature of the oligomeric state of DNA-bound gp59. The interactions of gp59 with single-stranded DNA, gp32, and gp41 all appear to be essential to load gp41 onto gp32-saturated single-stranded DNA, which may require the formation of a helicase loading complex consisting of gp59, gp32, and single-stranded DNA (*17*).

Gp59 has been shown to remain on the DNA after loading gp41 onto a forked DNA in the presence of adenosine 5′-*O*-3-thiotriphosphate (ATPγS) (*13*). Electron microscopy studies have found that gp32-covered single-stranded DNA on the lagging-strand template is organized into bobbin like structures that may also contain gp59 (*18*). However, it is unclear whether gp59 continues to travel with the helicase or dissociates from it and the fork in the presence of ATP. The fork-bound gp41 has been shown to functionally couple with the holoenzyme and to facilitate processive incorporation of nucleotide in a strand-displacement DNA synthesis by the holoenzyme (*19*). Such helicase-dependent DNA synthesis, however, does not require gp59 (*20*, *21*).

In *Escherichia coli (E. coli)*, a binding study of helicase loading at *oriC* suggests that the helicase loading protein DnaC is not retained with helicase DnaB at *oriC* after helicase loading (*22*). This is also consistent with the inability to detect any complexes formed between DnaC with DnaA and/or DnaB at *oriC* by electron microscopy (*23*). Likewise, DnaC does not remain in the assembled primosome on the single-stranded DNA genome of the ΦX174 phage (*24*, *25*).

Another property associated with gp59 is its inhibition of the elongation of various DNA substrates by the T4 holoenzyme in the absence of gp41 (*5*, *6*, *17*, *26*). We have demonstrated that such inhibition of the leading-strand holoenzyme progression by gp59 is the result of a complex formed between gp59 and gp43 on DNA, which is instrumental in preventing premature replication during the assembly of the T4 replisome (*1*). This inhibition can be rationalized in terms of a structural model in which the C-terminal helical domains of gp59 are inserted into the interface created by the thumb and exonuclease domains of gp43. This insertion effectively locks the enzyme into a conformation where switching of the 3′ end of DNA substrate between the polymerase and exonuclease domains is prevented. Consequently, both the polymerase and 3′ to 5′ exonuclease activities of gp43 are totally inhibited. Thus, continued assembly of the replisome through addition of the primosome components and elements of the lagging-strand holoenzyme can occur without the leading-strand replication.

In this work, we demonstrate that gp41 is capable of disrupting the gp43−gp59−DNA complex which allows gp59 to dissociate from the replication fork. This, occurring as a part of gp41 loading, restarts the stalled replication forks and initiates a helicase-dependent DNA synthesis. We also establish that the fork-bound gp41 is capable of recruiting the primase gp61 in the absence of gp59 to complete the primosome followed by functional replisome assembly. Finally, we clarify the role of gp59 during active replication

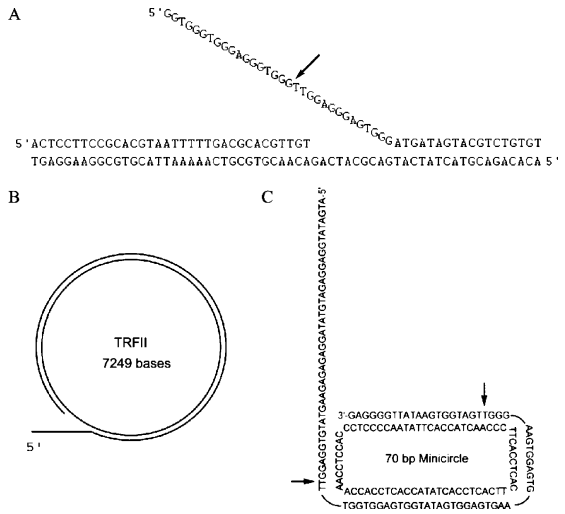

FIGURE 1: DNA substrates employed in functional assays. (A) The forked DNA substrate (34/62/50mer) is prepared from a 34-mer primer annealed to a 62-mer leading-strand template and a partially complementary 50-mer lagging-strand template with a priming site-(5′-GTT-3′) as indicated by an arrow. Strand displacement could be measured accurately by using this substrate without the need to involve additional proteins such as accessory proteins (gp45 and gp44/62) and single-stranded binding protein (gp32). (B) The tailed replicative form II (TRFII) M13 DNA substrate is a forked double-stranded M13 DNA substrate with a 43-mer lagging-strand that is created from elongation of a 73-mer oligonucleotide (5′-$(T)_{43}$-GATGTCCGCAACATCAAACATGACCACTGC-3′) whose 30 3′ nucleotides are annealed to the M13mp18 single-stranded DNA plasmid with a size of 7249 bases. (C) The 70-mer minicircle substrate is constructed by annealing a 109-mer oligonucleotide DNA to a circular 70-mer DNA. This template contains two priming sites (5′-GTT-3′) as indicated by the arrows. The design of the minicircle substrate allows the specific incorporation of radiolabeled ^{32}P-dGTP and ^{32}P-dCTP into the leading and lagging strand, respectively.

by showing that the absence of gp59 from a T4 replisome does not have any effect on the cycles of repetitive lagging-strand synthesis and the coupling between leading- and lagging-strand DNA syntheses.

MATERIALS AND METHODS

All fluorescence dyes were purchased from Molecular Probes. [γ-^{32}P]ATP, [α-^{32}P]dGTP and [α-^{32}P]dCTP were purchased from New England Nuclear. Unlabeled deoxyribonucleotides and ribonucleotides were purchased from Roche Biochemicals. Bacteriophage T4 proteins: exonuclease deficient gp43 (gp43(exo-)) (*27*), gp44/62 (*28*), gp45 (*29*), gp32 (*30*), gp41 (*16*), gp59 (*31*), and gp61 (*32*) were purified as previously described. All DNA substrates (Figure 1) were prepared according to the procedures described previously (*1*, *30*). A biotinylated forked DNA substrate (34/62/bio50mer) was prepared as above but with a 3′ end biotinylated 50-mer lagging-strand template of the same sequence (Integrated DNA Technologies, Inc.). All other chemicals were of analytical grade or better.

Protein Labeling. The fluorescent label Alexa Fluor 488 C_5 maleimide (A488), or Alexa Fluor 555 C_2 maleimide (A555) was attached to the accessible cysteine residue on gp59, gp41, and gp61 as required; Alexa Fluor 488 carboxylic acid, succinimidyl ester (A488) was attached to the N terminus of gp43. All labeling and characterization of the labeled proteins followed the procedures described previously (*1*, *33*).

Functional Assay of gp43 Polymerase Activity on the Small Forked DNA. A forked DNA substrate 34/62/50-mer (Figure 1A) with a 5′-^{32}P phosphate labeled primer strand (*1*), was preincubated with gp43(exo-) and gp59 at 25 °C for 2 min. To this was added gp41 if required and the reaction was then incubated at 25 °C for 1 min, followed by the addition of dNTPs. The typical final reaction mixture with a total volume of 12 μL contained 100 nM DNA substrate, 150 nM gp43, 1.2 μM gp59 and 1.8 μM gp41 in the polymerization buffer (25 mM HEPES, pH7.5, 8 mM $Mg(OAc)_2$, 40 mM NaOAc, 1 mM ATP, 5 mM DTT) with 250 μM dNTPs. The reaction was allowed to proceed for 30 s at 25 °C and then quenched with an equal volume of 0.3 mM ethylenediamine tetraacetic acid, disodium salt (EDTA) in loading dye with 1% sodium dodecyl sulfate (SDS). The mixture was separated by electrophoresis on a 12% denaturing polyacrylamide gel followed by phosphorimaging analysis. The progress of each reaction was determined by quantifying the amount of the remaining primer.

Functional Assay of gp43 Polymerase Activity on the TFRII M13 DNA Substrate. The tailed replicative form II (TRFII) M13 DNA substrate (Figure 1B) was synthesized as previously described (*34*). Replication reactions were carried out in a complex buffer containing 25 mM Tris-acetate (pH 7.5), 125 mM potassium acetate, and 10 mM magnesium acetate. The final reaction (60 μL) typically contains 2 nM TRFII DNA substrate, 16 nM gp43(exo-), 100 nM gp45 (as trimer), 18 nM gp44/62, 4 μM gp32, 200 nM gp59, 200 nM gp61, and 300 nM gp41, 1 mM ATP, 50 μM each dATP, dGTP, dCTP, and dTTP; 50 μM each GTP, CTP, and UTP; and [α-^{32}P]dCTP [3,000 Ci/mmol]. For each reaction, the holoenzyme was first allowed to assemble onto the DNA at 37 °C for 30 s, followed by the addition of gp32. The mixture was incubated at 37 °C for 2.5 min, and the reaction was initiated with the addition of dNTPs. Gp59 was added 1 min after the start of the reaction. Reaction aliquots were withdrawn at 2, 4, 6 and 8 min relative to the addition of dNTPs, quenched with an equal volume of 0.5 mM EDTA in gel loading buffer (30% glycerol, 0.25% bromophenol blue and xylene cyanol FF) and separated by electrophoresis on a 0.6% alkaline agarose gel, followed by phosphorimaging analysis. In reactions where the late addition of gp41 was required, gp41 was introduced 4 min after the addition of gp59, and the reaction aliquots were withdrawn at 5.5, 6, 8, 10 and 12 min relative to the addition of dNTPs. In the reactions where the late addition of gp61 was required, gp61 was added 2 min after the addition of gp41, and the reaction aliquots were withdrawn at 8, 10, 12 and 14 min relative to the addition of dNTPs. The amount of the strand-displacement synthesis and the leading- and lagging-strand synthesis for each reaction was quantified by Quantity One (BioRad) and analyzed by Origin 5 (MicroCal, Inc.).

Single-Molecule FRET. Single molecules were observed with a home-built fluorescence microscope using total internal reflection optics. The microscope filters were set to observe fluorescence from three different sources: F1: emission from donor A488 (excitation at 488 nm/emission at 510−540 nm), F2: emission from energy transfer between A488 and A555 (excitation at 488 nm/emission at 595−645 nm), and F3: emission from acceptor A555 (excitation at 514 nm/emission at 535−585 nm). Experiments were performed at ambient temperature, ∼25 °C as reported in detail previously (*1*, *33*). All single-molecule experiments were performed in triplicate, and in all cases well-resolved single-molecule fluorescent spots were observed.

The forked DNA (34/62/bio50-mer, Figure 1A, with a 3′ end biotinylated 50-mer) was attached to a glass slide prepared with avidin on the surface as described previously (*1*). Individual forked DNA molecules coated with fluorescently labeled proteins were observed as well-separated fluorescent spots in the microscope field. A solution of the first protein to be added in a given experiment was passed over a slide with bound forked DNA substrate three times and allowed to stand for 10 min. Depending on the experiment, 100 nM fluorophore-labeled or unlabeled protein in Tris buffer was used. The protein not bound to the forked DNA was then washed away with three aliquots of buffer. Subsequent protein or reagent additions were carried out on the microscope stage without moving the slide in three similar applications. This served to wash away the previous unbound protein and only an excess of the final protein or reagent was left on the slide. Fluorescence spots are observed only in the presence of biotinylated forked DNA substrate, demonstrating that nonspecific binding of proteins to the slide does not occur.

Effect of gp59 Concentration on Lagging-Strand Synthesis. Replication reactions were carried out in the same complex buffer as described above. The standard replication conditions used in all minicircle reactions consisted of 100 nM minicircle substrate (*30*) (Figure 1C), 240 nM each of gp43(exo-), gp45 (as trimer), and gp44/62, 600 nM each of monomer gp41 and gp61, 4.5 μM of gp32, 100 μM each of CTP, GTP, and UTP, 2 mM ATP, and 100 μM each of dATP, dGTP, dCTP, and dTTP in a typical reaction volume of 25 μL. [α-^{32}P]dGTP and [α-^{32}P]dCTP (3000 Ci/mmol) were included to monitor the leading- and lagging-strand synthesis, respectively. The proteins for holoenzyme assembly (gp43(exo-), gp45, and gp44/62) were first preincubated at 37 °C with the minicircle DNA template in the presence of 2 mM ATP for 30 s followed by the addition of the primosome proteins (gp41 and gp61) and gp32 along with dNTPs, rNTPs, and 2 mM ATP. The reaction was then allowed to proceed for 1 min before the addition of radioactive [α-^{32}P]dGTP or [α-^{32}P]dCTP. Ten microliter aliquots were removed at 30, 60, 90, 120 and 150 s and quenched with an equal volume of 0.3 M EDTA in gel loading buffer. Reaction products were separated by electrophoresis on a 0.8% alkaline agarose gel followed by phosphorimaging analysis. Standard DNA replication reactions were carried out at various gp59 concentrations (600, 100, 10 and 0 nM). [α-^{32}P]dCTP (3000 Ci/mmol) was included in the reactions for the detection of the lagging-strand synthesis and was added 1 min after the initiation of the reaction. More [α-^{32}P]dCTP was introduced into the reactions with lower concentrations of gp59 because a lower number of active forks were expected. The reactions were allowed to proceed for another 3 min before quenched in an equal volume of pH 8.0, 0.3 M EDTA in gel loading buffer. Reaction products were separated by electrophoresis on a 0.8% alkaline agarose gel and followed by phosphorimaging analysis.

Coordinated Strand Synthesis in the Absence of gp59. A total of four reactions were carried out as described above for standard minicircle DNA replication reactions. [α-^{32}P]-dGTP was included in reactions 1 and 2 for measuring the leading-strand synthesis, and [α-^{32}P]dCTP was included in

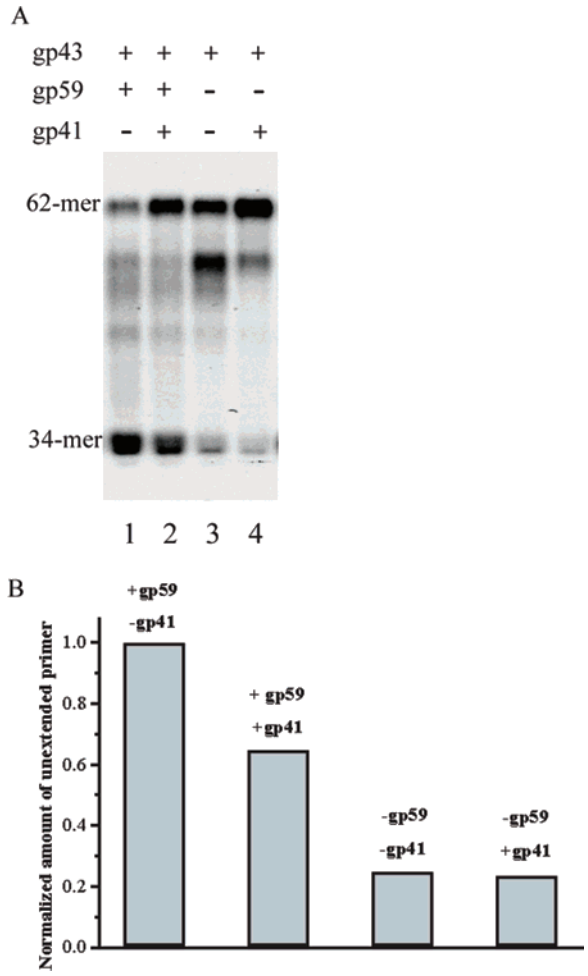

FIGURE 2: The inhibition of gp43 polymerase activity by gp59 on a small forked DNA substrate (Figure 1A) can be rescued by gp41. (A) The results of strand-displacement reactions by gp43(exo-) in the presence and absence of gp59 and gp41. ^{32}P-labeled 34-mer primers of the DNA substrate for the strand-displacement reaction and the corresponding ^{32}P-labeled 62-mer products are shown on a 12% denaturing polyacrylamide gel. (B) The normalized amount of unextended primer in each reaction, determined from panel A, is displayed in a column graph.

reactions 3 and 4 for measuring the lagging-strand synthesis. Gp59 was omitted from all four reactions. Gp41 was further omitted from reactions 2 and 4, but was present in reactions 1 and 3.

RESULTS

The Inhibition of gp43 Polymerase Activity by gp59 Can Be Rescued by gp41 on a Small Forked DNA Substrate. Previously, we reported a functional assay of polymerase activity in the format of a primer-elongation reaction (strand-displacement) on a small forked DNA substrate (*1*). Using the same assay, the effect of gp41 on restoring the polymerase activity in the presence of gp59 was investigated. The amount of unextended primer (34-mer) can be used to measure the amount of the remaining unreactive gp59−gp43−DNA complex. As depicted in Figure 2B, the presence of gp41 (MgATP) causes a 40% decrease in the amount of the inhibitory complex (reaction 2) from the initial complex in the absence of gp41 (reaction 1). The majority of extended primer shown in reaction 2 in Figure 2A is the full-length product (62-mer), which is usually observed from the reactions in the absence of gp59, indicated in the control reactions 3 and 4 in Figure 2A. The bands that are smaller than full-length product are partially extended primers, which become more significant in the absence of gp41 (reaction 3). We attribute the effect of gp41 to a specific interaction between gp41 and gp59 on the lagging-strand DNA that disrupts the interaction between gp43 and gp59 and restores the gp43 activity.

The Inhibition of gp43 Polymerase Activity by gp59 Can Be Rescued by gp41 on a TRFII M13 DNA Substrate. Strand-displacement DNA synthesis was performed on a tailed replicative form II (TRFII) M13 DNA substrate (Figure 1B) in the presence of holoenzyme and gp32, which is a close mimic of helicase-independent leading-strand synthesis. The extension of the leading-strand primer from an initial size of 7.2 kb was revealed by the incorporation of radiolabeled ^{32}P-dCTP, after separation of the extension-reaction products by alkaline agarose gel electrophoresis (Figure 3A). Forks in the absence of gp59 were shown previously to display a continuous progression (*1*), while the progression of the forks in the presence of gp59, which was introduced 1 min after initiation of the reaction, was stalled after a 3-min reaction time and showed very little change at later times (Figure 3A). The stalling of the replication forks derived from a very stable ternary complex formed by gp43, gp59, and the replication fork (*1*). Five minutes after gp41 was introduced into the reaction mixture, a fraction of the stalled forks was restarted leading to the helicase-dependent leading-strand synthesis on those forks, as demonstrated by newly synthesized DNAs with sizes greater than 23 kb and an estimated fork rate of greater that 190 nucleotide/s (Figure 3A). The amount of initially stalled forks diminished over time and leveled off after 3 min. This diminution followed an exponential rate law with a half time of about 0.61 ± 0.04 min (Figure 3B). These results suggest that the time delay reflects the time required for gp41 to load onto the fork and to disrupt the inhibiting gp43−gp59−DNA complex, thus initiating helicase-dependent DNA synthesis. Seven minutes after the addition of gp41, about 60% of initially stalled forks remained stalled and most likely represent aborted forks that have been previously observed in such replication assays.

Gp61 Can Be Loaded onto a Fork That Is Carrying Out a Helicase-Dependent DNA Synthesis To Form a Functional Replisome on a TRFII M13 DNA Substrate. The effect of gp61 on the fork carrying out helicase-dependent DNA synthesis was investigated on a TRFII M13 DNA substrate (Figure 1B) in the presence of holoenzyme, gp32, gp59, and gp41. As described above, the helicase-dependent DNA synthesis produced long lengths of single-stranded DNAs without any observable Okazaki fragments because of the absence of the RNA primer required for the lagging-strand DNA synthesis. By introducing gp61 into such a reaction, DNAs with sizes smaller than the M13 template (7.2 kb) were obtained (Figure 3A). Analyzing the sizes of these DNAs revealed two fractions of DNA fragments, both with increasing intensities over time, one with constant sizes (2.8 kb) and the other with increasing sizes (3.0 kb to 4.0 kb) during the same period of time (Figure 3A and 3C). The fraction with constant sizes represents Okazaki DNA fragments produced by a fully functional replisome that was most likely assembled when the fork-bound gp41 recruited gp61 from solution to form an active primosome, along with assembly of the lagging-strand holoenzyme to complete assembly of the functional replisome. The size of Okazaki

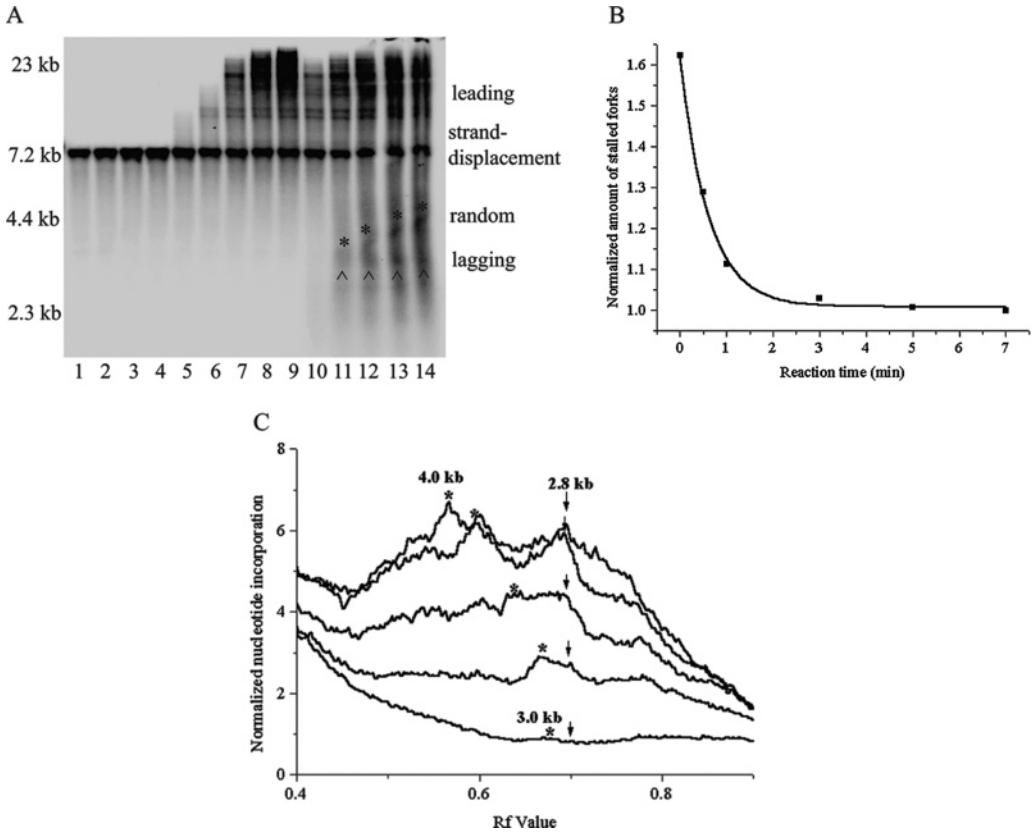

FIGURE 3: The inhibition of gp43 polymerase activity by gp59 can be rescued by gp41 on a TRFII M13 DNA substrate, and the functional replisome can be assembled by the subsequent addition of gp61. (A) The results of the extension of the leading-strand primer (lanes 1 to 14) and the RNA primer (lanes 9 to 14) by the incorporation of radiolabeled ^{32}P-dCTP are shown on an alkaline agarose gel. For the reactions in lanes 1 to 4 (absence of gp41), the holoenzyme was allowed to assemble onto the DNA at 37 °C for 30 s, followed by the addition of gp32. The mixture was incubated at 37 °C for an additional 2.5 min, and the reaction was initiated with the addition of dNTPs. Gp59 was added 1 min after the initiation of the reaction. Reaction aliquots were withdrawn at 2, 4, 6 and 8 min relative to the addition of dNTPs, corresponding to lanes 1 to 4. The reactions in lanes 5 to 9 (presence of gp41) were initiated as reactions 1 to 4, followed by the addition of gp41 4 min after the addition of gp59. Reaction aliquots were withdrawn at 5.5, 6, 8 10 and 12 min relative to the addition of dNTPs, shown in lanes 5 to 9. For the reactions in lanes 10 to 14 (presence of gp61), gp61 was added 2 min after the addition of gp41. Reaction aliquots were withdrawn at 8, 10, 12, 14 and 16 min relative to the addition of dNTPs. "Leading" represents the leading-strand synthesis; "strand-displacement" represents the helicase-independent DNA synthesis; "random" represents the random primer extension (the band is labeled with *****); and "lagging" represents the Okazaki fragment synthesis (the band is labeled with ∧). (B) Effect of gp41 on the inhibition of gp43 by gp59. The band intensities representing the strand-displacement DNA synthesis in the presence of gp41, in lanes 5 to 9 in panel A, are plotted as a function of reaction time relative to the addition of gp59. All the intensities are normalized to an arbitrary value. Because of the inhibition by gp59, the amount of products from reaction 2 to 4 varied by very little; therefore, their band intensities represent the amount of stalled forks. The band from reaction 3 is used as the initial data point ($t = 0$). After the addition of gp41, the amount of stalled forks decreases as a function of time and follows a single-exponential curve, with a half time of about 0.61 ± 0.04 min. (C) Two fractions of DNA fragments. The one with a constant size (2.8 kb, marked with arrows) represents the products of the Okazaki DNA fragment synthesis; the other with various sizes (3.0 kb to 4.0 kb, marked with *****) represents the products of the random RNA primer extension. The Rf values are defined as the ratio between the migrated distances and the length of the gel. The intensities of the bands are normalized to an arbitrary value.

DNA fragments was greater than the typical size of Okazaki fragments (2.5 kb) under similar condition (*34*) but with all the proteins introduced at the beginning of the reaction. Presumably, when gp61 was introduced 2 min after initiation of helicase-dependent leading-strand DNA synthesis, a long single-stranded lagging-strand DNA template already had been produced that would likely trap a significant amount of gp32 present in solution, resulting in longer Okazaki fragments as has been reported previously (*30*, *35*). The other fraction of DNA fragments with increasing sizes likely represents the products from random RNA primer extension reactions on the same single-stranded lagging-strand DNA template (*36*). Although such extension reactions involved all the proteins required by normal lagging-strand synthesis, they seemed to be uncoupled from the leading-strand synthesis as indicated by their size variation.

The Interaction between gp43 and gp59 Can Be Disrupted by gp41 Leading to Dissociation of gp59 from the Fork as Observed by Single-Molecule FRET. As described previously (*1*), the functional properties of the gp43−gp59−DNA complex were demonstrated by single-molecule fluorescence microscopy that measured fluorescence resonance energy transfer (FRET) on single forked DNA molecules (34/62/bio50-mer, Figure 1C) whose 3′ lagging-strand (50-mer) ends were immobilized on a microscope glass slide (*1*). The same technology also allowed us to study the effect of gp41 on the gp43−gp59−DNA complexes. In Figure 4, the presence of A488-labeled gp43(exo-) bound to single molecules of the forked DNA is displayed in frame j with filter set 1 (F1), whereas the presence of A555-labeled gp59 bound to single molecules of the forked DNA is displayed in frames c, f, i and l with F3. FRET between donor/acceptor pairs (A488-

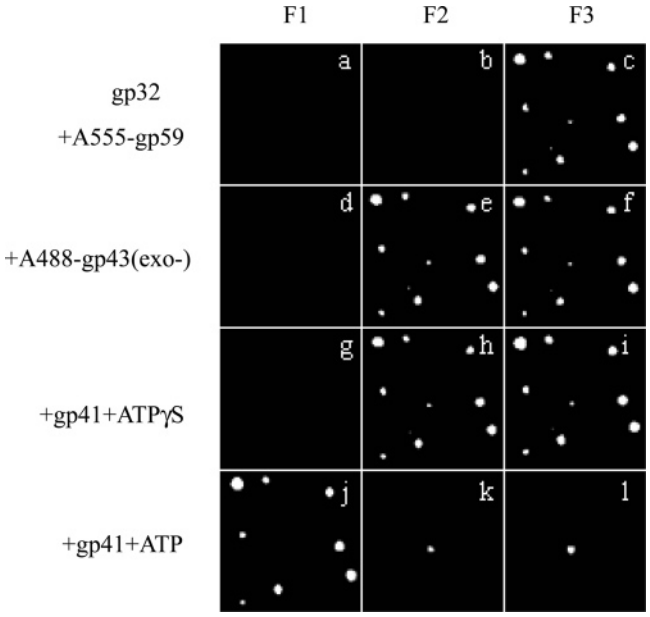

FIGURE 4: The results of single-molecule FRET experiments on a set of immobilized single forked DNA molecules (34/62/bio50-mer) whose 3′ lagging-strand (50-mer) ends were immobilized on a microscope glass slide. The fluorescence from individual molecules of DNA with the proteins bound in the order as indicated at the side of each row. The microscope filters were set to observe fluorescence from three different sources: F1: emission from donor A488 (excitation at 488 nm/emission at 510−540 nm), F2: emission from energy transfer between A488 and A555 (excitation at 488 nm/emission at 595−645 nm), and F3: emission from acceptor A555 (excitation at 514 nm/emission at 535−585 nm). MgATPγS and MgATP (500 μM) were present during measurements displayed in frames g−i and frames j−l, respectively. The presence of gp59 bound to each forked DNA molecule in the presence of gp32 is displayed in frames c, f, i and l. When A488-gp43(exo-) was added to the mix, A488-gp43(exo-) formed a complex with A555-gp59, detected by the FRET in frame e. Such a complex could not be disrupted by gp41 if the non-hydrolyzable analogue ATPγS was present. When gp41 was introduced with ATP, the ternary complex was disrupted, shown by disappearance of the FRET between A488-gp43(exo-) and A555-gp59 in frame k. Gp59 also dissociated from the fork as displayed in frame l.

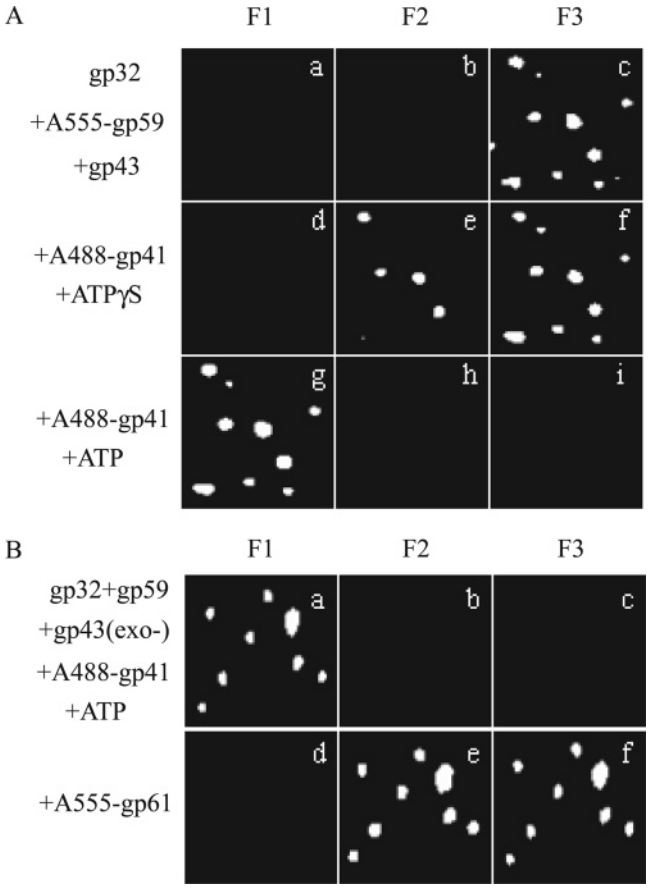

FIGURE 5: The results of additional single-molecule FRET experiments under the same conditions described in Figure 4. The fluorescence from individual molecules of DNA with the proteins bound in the order as indicated at the side of each row. (A) A555-gp59 is bound to the forked DNA as displayed in frame c. The addition of A488-gp41 in the presence of ATPγS produces a protein complex between A488-gp41 and A555-gp59, displayed as a FRET in frame e with F2. When A488-gp41 is added in the presence of ATP, the helicase remains on the fork (frame g) but gp59 is no longer associated with the fork (frame i). (B) The fork-bound A488-gp41 (frame a) in the presence of gp32, gp59 and gp43 is shown to be capable of recruiting A555-gp61 from the solution and loading it onto the forked DNA (frame f) to form a complex revealed by the FRET (frame e) between A488-gp41 and A555-gp61.

gp43(exo-) and A555-gp59) on each forked DNA molecule is observed with F2 in frames e, h and k, suggesting intimate protein−protein contacts between gp43 and gp59 on the forked DNA. We have previously shown that labeled gp43(exo-) and gp59 bind independently to the DNA substrate and fluoresce (*1*, *33*), therefore self-quenching of either labeled gp43 or gp59 is extremely unlikely. Thus, the absence of fluorescence in frame d indicates essentially complete energy transfer of the fluorophore A488 on gp43(exo-) to A555 on gp59, within the sensitivity of the experiment.

When gp41, along with 500 μM of MgATP, was introduced, virtually all of the single molecules in frames e and f or h and i detected by F2 and F3, respectively, disappear, indicating that gp59 dissociates from the gp43−gp59−DNA complex and is no longer bound to the forked DNA. The identical phenomenon was also observed in the absence of gp32 (data not shown), suggesting that gp32 is not required for the dissociation of gp59 from the gp43−gp59−DNA complex by gp41. The dissociation of gp59 is an ATP-driven process, and disappearance of gp59 is not observed when the non-hydrolyzable analogue ATPγS is used (frames h and i), which is consistent with our result from the ensemble FRET experiment (data not shown) and the previous report that gp59 remains associated with the forked DNA after loading gp41 in the presence of ATPγS (*13*). The presence of A488-labeled gp43(exo-) with F1 in frame j indicates that gp43 remains on the forked DNA, likely along with newly loaded gp41. The one remaining single molecule in frames k and l might result from incomplete dissociation of gp43−gp59 complex. Since gp43 remains on the DNA substrate, gp41 apparently is unable to completely unwind the fork substrate. We attribute this to the slide surface being very close to the end of the fork and acting to block gp41 from translocating through the duplex region of the fork.

Gp59 While Complexed to gp43 Retains Its Ability To Load gp41 and To Initiate the Subsequent Assembly of the Primosome in a Stepwise Fashion as Observed by Single-Molecule FRET. The loading of gp41 by gp59 alone on small forked DNA substrates has been demonstrated previously by functional assays (*13*, *15*) as well as by single-molecule experiments (*33*). In Figure 5A, we are able to visualize the

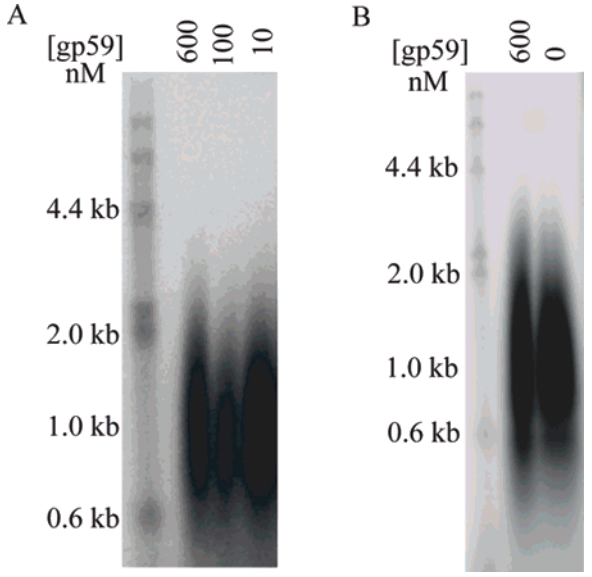

FIGURE 6: Gp59 has no effect on the size of the Okazaki fragments during the lagging-strand synthesis. Standard lagging-strand DNA replication reactions on a minicircle DNA substrate are shown on 0.8% alkaline agarose gels. Reactions were carried out at various gp59 concentrations (600, 100, 10, and 0 nM). [α-^{32}P]dCTP (3000 Ci/mmol) was included in the reactions for the detection of the lagging-strand synthesis and was added 1 min after the initiation of the reaction. More [α-^{32}P]dCTP was introduced into the reactions with lower concentrations of gp59 because a lower number of active forks were expected. The reactions were allowed to proceed for another 3 min before quenched. Reaction products were analyzed by electrophoresis on a 0.8% alkaline agarose gel and followed by phosphorimaging. (A) The effect of various concentrations of gp59 on the lagging-strand synthesis. All reactions show identical sizes (1.0 kb) of the lagging-strand synthesis. (B) The effect on the lagging-strand synthesis in the presence of gp59 (600 nM) compared to in the absence of gp59. Both display identical sizes (1.0 kb) of the lagging-strand DNA synthesis.

loading of gp41 by gp59 in a more biologically relevant system, where gp59 is complexed to gp43(exo-) on a forked DNA substrate in the presence of gp32, indicated by DNA-bound A555-gp59 in frame c. When A488-gp41 was introduced along with ATPγS, a small fraction of gp41 was loaded onto the fork and complexed with gp59, indicated by the FRET between A555-gp59 and A488-gp41, displayed in frame e with F2. Apparently, gp59 is inefficient in the loading of gp41 in the presence of ATPγS and no dissociation of gp59 is observed under this condition (frame f), consistent with the result described above. When 500 μM MgATP was added, the presence of A488-gp41 was observed on the fork (frame g) but gp59 has now dissociated (frame i). This result when combined with the observation that gp43 remains on the fork after gp59 dissociates is consistent with the presence of both gp43 and gp41 on the fork as a protein complex to carry out helicase-dependent DNA synthesis.

In a separate experiment (Figure 5B), where A488-gp41 was pre-loaded on the fork as described in Figure 5A, such fork-bound gp41 is shown to be capable of recruiting gp61 from the solution and loading it onto the forked DNA as documented in frame f. The FRET between A555-gp61 and A488-gp41 verifies the existence of a protein−protein interaction between gp61 and gp41 within the primosome. The single-molecule frames presented (Figures 4 and 5) are examples of typical data, similar results have been obtained for hundreds of molecules.

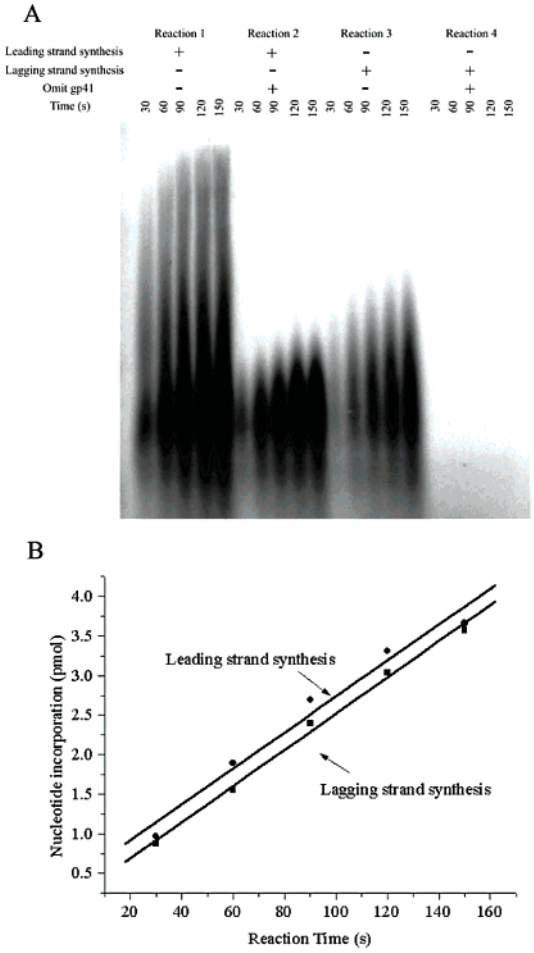

FIGURE 7: A fully coupled leading- and lagging-strand DNA synthesis in the absence of gp59. (A) Standard DNA replication reactions on a minicircle DNA substrate are shown on 0.8% alkaline agarose gel. Aliquots were removed at 30, 60, 90, 120, and 150 s. A total of four reactions were carried out. [α-^{32}P]dGTP was included in reactions 1 and 2 for measuring the leading-strand synthesis, and [α-^{32}P]dCTP was included in reactions 3 and 4 for measuring the lagging-strand synthesis. Gp59 was omitted from all four reactions. Gp41 was omitted from reactions 2 and 4, but was present in reactions 1 and 3. Reaction 1 represents the sum of the helicase-dependent leading-strand synthesis and the strand-displacement synthesis; reaction 2 represents only the strand-displacement synthesis; reaction 3 represents the total lagging-strand synthesis; reaction 4 serves as a control and shows that there is no lagging-strand synthesis in the absence of gp41 helicase. (B) The helicase-dependent leading- and lagging-strand DNA syntheses are coupled in the absence of gp59. The rate of the leading-strand synthesis is determined by subtraction of reaction 2, representing the strand-displacement synthesis (absence of gp41) from reaction 1, which includes both the leading-strand synthesis (helicase-dependent) and the strand-displacement synthesis (helicase-independent). The rate of the lagging-strand synthesis is determined by subtraction of reaction 4, representing the amount of the lagging-strand synthesis in the absence of gp41 from reaction 3, which represents the total lagging-strand synthesis. Identical rates are shown for both the leading- and lagging-strand synthesis in the absence of gp59.

Gp59 Is Not Required during DNA Replication on the Minicircle Substrate. The possible roles of gp59 in lagging-strand synthesis were investigated by carrying out DNA replication on the minicircle substrate (Figure 1C). This system allowed the assembly of a fully functional primosome in the absence of gp59 although with much lower efficiency, as described previously (*30*). One characteristic feature of a normal lagging-strand synthesis is the ability of the replisome

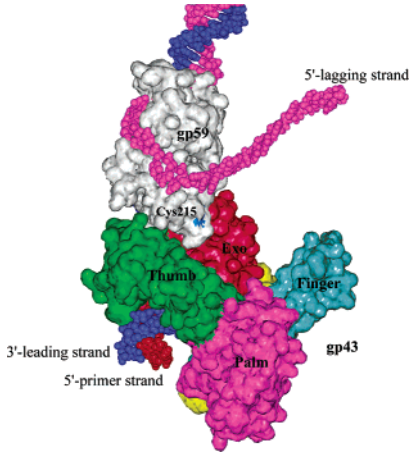

FIGURE 8: A model of the gp59−gp43−forked DNA ternary complex. The gp59−gp43 model (*1*) serves as the basis for the modeling of the ternary complex. The gp43-bound primed leading-strand DNA was modeled based on the X-ray crystal structure of the homologous RB69 polymerase complexed with a primer−template DNA (*39*). The gp59-bound fork DNA was modeled based on the structural similarity of gp59 to the high mobility group protein (HMG) (*12*), where the N-terminal domain of gp59 makes close contact with the fork region of the DNA and the lagging strand transverses the hydrophobic inter-domain groove and extends into the bulk solvent. The primed leading-strand DNA and the fork were connected based on the trajectory suggested by the RB69 DNA polymerase ternary complex structure and the surface topology of both gp43 and gp59. The rendered protein surfaces of gp59 and gp43 are colored as follows: for gp43, the N-terminal domain (residues 1−108 and 340−382) is in yellow, the exonuclease domain (residues 109−339) in red, palm (residues 383−468 and 573−729) in magenta, fingers (residues 469−572) in cyan and thumb (residues 730−898) in green; gp59 is in gray. The forked DNA is shown as a CPK model. The template strand is colored in blue; the single-stranded lagging-strand is colored in magenta; and the primer strand is colored in red. The previously identified cross-linking site Cys215 of gp59 is colored in sea blue.

to maintain a size distribution of the Okazaki fragments centered around 1.0 kb. When a crucial protein element is missing from the replisome, the regular pattern of repetitive lagging-strand synthesis will be disrupted due to interference with the replisome remodeling process (*30*). This generally results in an increase in the Okazaki fragment size due to a delay in utilization of RNA primers by the lagging-strand polymerase. When the concentration of gp59 was decreased from 600 nM to 100 nM and then to 10 nM, no obvious change in the size of Okazaki fragments was observed (Figure 6A). This result suggests that either gp59 is not required for lagging-strand synthesis, or it is a highly processive replisome component. We then measured the size of the lagging-strand product in the absence of gp59 to distinguish between these two possibilities. As shown in Figure 6B, the size of the Okazaki fragments remains constant whether or not there is any gp59 in the reaction, indicating that gp59 does not play a significant role in the repetitive cycles of lagging-strand synthesis, such as primer hand-off, reassembly of the holoenzyme, etc., which would otherwise result in the increase in the size of the Okazaki fragments due to the delay of the primosome remodeling process during the lagging-strand synthesis (*37*). It also follows that the recruitment of the dissociative gp61 primase from solution to form the primosome does not require the presence of gp59. One would expect, if gp59 acted to facilitate gp61 loading, then the size of the Okazaki fragments would have dramatically increased at low concentrations of gp59 because of a decreased gp61 association rate resulting in reduced priming frequency (*37*).

The effect of gp59 on the entire replisome was also evaluated by studying both leading- and lagging-strand DNA synthesis in the absence of gp59. The replisome is sometimes regarded as a protein machine that carries out efficient DNA synthesis through the coordination of an intricate protein interaction network. Defects within this network will ultimately affect the coupling between the leading- and lagging-strand syntheses. To test whether gp59 is required for maintaining the coupled synthesis, we measured the rate of leading- and lagging-strand synthesis independently on a minicircle substrate (Figure 7A). As shown in Figure 7B, helicase-dependent DNA replication remains coupled even when gp59 is omitted from the reaction mixture. Taken together, our data argue against a role for gp59 in leading- and lagging-strand synthesis, or a role in coordinating these two syntheses during replication. Therefore, it is probable that gp59, after assembly of the replisome, is no longer required as an active component within the replisome during DNA synthesis.

DISCUSSION

These results, coupled with those previously reported (*1*) indicate that the replication process is regulated by gp59 and gp41, with gp59 locking the leading-strand holoenzyme and gp41 unlocking it. We believe that the generation of a gp59−gp43−DNA ternary complex is absolutely required in recombination-dependent replication in the bacteriophage T4 system. This intermediate complex ensures an ordered and controlled pathway for assembly of all three replisome units by preventing premature replication by the leading-strand holoenzyme (*1*).

Because the fork-bound gp41 alone is capable of promoting leading-strand DNA synthesis by functionally coupling to the leading-strand holoenzyme in the absence of gp59 (*19*, *21*, *38*), it is reasonable to believe that gp41 loading by gp59 may trigger the restart of stalled replication forks by disruption of the inhibitory effect of gp59 on gp43. Our experimental results confirm this hypothesis: gp41 is able to restart a completely stalled replication fork by displacing gp59 from the inhibiting gp59−gp43−DNA complex and subsequently to initiate helicase-dependent DNA synthesis by forming the functional replicative complex gp41−gp43−DNA. The loading of gp41 by a DNA-bound gp59 is consistent with the hypothesis that helicase loading occurs in a stepwise fashion, where gp59 binds to the forked DNA structure, then serves as a scaffold for gp41 binding through its interaction with the C terminus of gp41 (*13*). Subsequently the hexameric helicase ring assembles around the lagging-strand DNA and gp59 dissociates from DNA.

Since helicase loading does not necessarily require ATP hydrolysis, the requirement of ATP for gp59 dissociation suggests that ATP hydrolysis by gp41 likely drives this process, which may require the translocation activity of helicase. The finding of bobbin-like structures that may contain gp59 observed by electron microscopy on the lagging-strand template of T4 replication forks (*18*), does not refute our observation that gp59 does not remain with the final replisome, because such structures could arise from aborted forks, nonspecific binding between gp59 and gp32

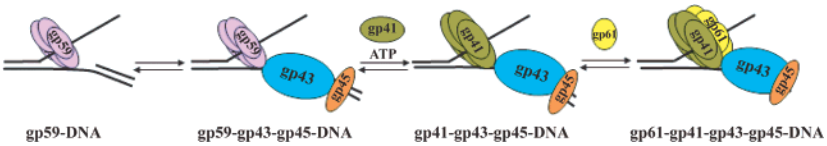

FIGURE 9: A stepwise pathway for T4 leading-strand holoenzyme and primosome assembly. Gp59, gp41, and gp61 are all represented as hexameric ring forms encircling the lagging-strand DNA; gp45, the clamp protein, is shown with gp43 on the leading strand although the order of addition of these two proteins remains to be elucidated. The color scheme is as follows: gp59, lavender; gp43, sky blue; gp45, orange; gp41, green; gp61, yellow.

on gp32-covered single-stranded DNA, or helicase loading complexes formed between gp59 and gp32 prior to helicase loading (*17*).

We have developed a simplified model of a gp59−gp43−DNA ternary complex (Figure 8) based on the hypothetical model between gp59 and gp43 described previously (*1*). This would suggest that gp41 can readily access the lagging-strand DNA. The bound gp41 moves in the 5′ to 3′ direction along the lagging strand to contact the fork-bound gp59. A previous cross-linking study suggested that the Cys215 of gp59 interacts with the C terminus of gp41 (*16*). In our current model, the Cys215 residue of gp59 is well exposed, close to the lagging-strand DNA, and, therefore, is spatially accessible for gp41. The translocation of gp41 along the lagging strand that requires ATP hydrolysis will destabilize the binding of gp59−gp43−DNA complex so that gp59 dissociates. Although only the gp59 monomer is considered in our current model, the putative oligomeric structure of gp59 would retain similar interactions with both gp43 and gp41.

Following the formation of the functional coupling complex gp41−gp43−DNA, the fork-bound gp41 was shown to be capable of recruiting gp61 from solution without any requirement for gp59 to form an active primosome. The active primosome facilitates subsequent assembly of the final replisome that functions in Okazaki fragment synthesis, as shown by functional assays in Figure 3A and 3C. We presume, in vivo, that the full replisome is likely assembled in a stepwise fashion, initiated by gp59 binding to the fork region of a D loop containing a gp32-coated lagging strand. In this case, we suggest gp59 assists in assembly of the leading-strand holoenzyme, followed by loading of gp41, dissociation of gp59 and finally loading of gp61 to form primosome complex with gp41. A cartoon of the process is presented in Figure 9, where the hexameric ring structure of gp59 is employed to illustrate the fork-bound gp59 based on the hypothesis that the formation of the 1:1 gp43−gp59 complex on DNA is dependent on the formation of an oligomeric structure of gp59 on the fork (*1*). Only one subunit of the putative oligomeric structure of gp59 likely interacts simultaneously with both gp43 and gp41 in our current model. The completion of the leading-strand holoenzyme and the primosome along with the lagging-strand holoenzyme will result in a complete replisome.

Although gp59 plays an essential role in the T4 primosome assembly, its role in the active replication had not yet been defined. We show that the absence of gp59 from a T4 replisome does not have any effect on the cycles of repetitive lagging-strand DNA synthesis, does not affect the coupling between leading- and lagging-strand DNA synthesis, and has no effect on the rate of the leading-strand fork movement (*30*). We conclude that gp59 is not involved in replisome assembly beyond helicase loading and does not play a significant functional role during active replication.

REFERENCES

1. Xi, J., Zhuang, Z., Zhang, Z., Selzer, T., Spiering, M. M., Hammes, G. G., and Benkovic, S. J. (2005) Interaction between the T4 Helicase Loading Protein (gp59) and the DNA Polymerase (gp43): A Locking Mechanism to Delay Replication During Replisome Assembly, *Biochemistry 44*, 2305−2318.
2. Alberts, B. M. (1987) Prokaryotic DNA replication mechanisms, *Philos. Trans. R. Soc. London, Ser. B. 317*, 395−420.
3. Nossal, N. G. (1994) The bacteriophage T4 DNA replication fork, in *Molecular Biology of Bacteriophage* (Karam, J. D., Ed.) pp 43−55, ASM Press, Washington, DC.
4. Benkovic, S. J., Valentine, A. M., and Salinas, F. (2001) Replisome-mediated DNA replication, *Annu. Rev. Biochem. 70*, 181−208.
5. Jones, C. E., Mueser, T. C., and Nossal, N. G. (2004) Bacteriophage T4 32 protein is required for helicase-dependent leading strand synthesis when the helicase is loaded by the T4 59 helicase-loading protein, *J. Biol. Chem. 279*, 12067−12075.
6. Jones, C. E., Mueser, T. C., Dudas, K. C., Kreuzer, K. N., and Nossal, N. G. (2001) Bacteriophage T4 gene 41 helicase and gene 59 helicase-loading protein: a versatile couple with roles in replication and recombination, *Proc. Natl. Acad. Sci. U.S.A. 98*, 8312−8318.
7. Bleuit, J. S., Xu, H., Ma, Y., Wang, T., Liu, J., and Morrical, S. W. (2001) Mediator proteins orchestrate enzyme-ssDNA assembly during T4 recombination-dependent DNA replication and repair, *Proc. Natl. Acad. Sci. U.S.A. 98*, 8298−8305.
8. Barry, J. E., and Alberts, B. M. (1994) Purification and characterization of bacteriophage T4 gene 59 protein. A DNA helicase assembly protein involved in DNA replication, *J. Biol. Chem. 269*, 33049−33062.
9. Morris, C. F., Moran, L. A., and Alberts, B. M. (1979) Purification of gene 41 protein of bacteriophage T4, *J. Biol. Chem. 254*, 6797−6802.
10. Alberts, B. M. (1970) Function of gene 32-protein, a new protein essential for the genetic recombination and replication of T4 bacteriophage DNA, *Fed. Proc. 29*, 1154−1163.
11. Dong, F., Gogl, E. P., and von Hippel, P. H. (1995) The phage T4-coded DNA replication helicase (gp41) forms a hexamer upon activation by nucleoside triphosphate, *J. Biol. Chem. 270*, 7462−7473.
12. Mueser, T. C., Jones, C. E., Nossal, N. G., and Hyde, C. C. (2000) Bacteriophage T4 gene 59 helicase assembly protein binds replication fork DNA. The 1.45 Å resolution crystal structure reveals a novel alpha-helical two-domain fold, *J. Mol. Biol. 296*, 597−612.
13. Jones, C. E., Mueser, T. C., and Nossal, N. G. (2000) Interaction of the bacteriophage T4 gene 59 helicase loading protein and gene 41 helicase with each other and with fork, flap, and cruciform DNA, *J. Biol. Chem. 275*, 27145−27154.
14. Morrical, S. W., Hempstead, K., and Morrical, M. D. (1994) The gene 59 protein of bacteriophage T4 modulates the intrinsic and single-stranded DNA-stimulated ATPase activities of gene 41 protein, the T4 replicative DNA helicase, *J. Biol. Chem. 269*, 33069−33081.
15. Raney, K. D., Carver, T. E., and Benkovic, S. J. (1996) Stoichiometry and DNA unwinding by the bacteriophage T4 41:59 helicase, *J. Biol. Chem. 271*, 14074−14081.
16. Ishmael, F. T., Alley, S. C., and Benkovic, S. J. (2002) Assembly of the bacteriophage T4 helicase: architecture and stoichiometry of the gp41-gp59 complex, *J. Biol. Chem. 277*, 20555−20562.
17. Ma, Y., Wang, T., Villemain, J. L., Giedroc, D. P., and Morrical, S. W. (2004) Dual functions of single-stranded DNA-binding protein in helicase loading at the bacteriophage T4 DNA replication fork, *J. Biol. Chem. 279*, 19035−19045.

18. Chastain, P. D., Makhov, A. M., Nossal, N. G., and Griffith, J. (2003) Architecture of the replication complex and DNA loops at the fork generated by the bacteriophage T4 proteins, *J. Biol. Chem. 278*, 21276−21285.
19. Delagoutte, E., and von Hippel, P. H. (2001) Molecular mechanisms of the functional coupling of the helicase (gp41) and polymerase (gp43) of bacteriophage T4 within the DNA replication fork, *Biochemistry 40*, 4459−4477.
20. Jarvis, T. C., Ring, D. M., Daube, S. S., and vonHippel, P. H. (1990) "Macromolecular crowding": thermodynamic consequences for protein−protein interactions within the T4 DNA replication complex, *J. Biol. Chem. 265*, 15160−15167.
21. Schrock, R. D., and Alberts, B. (1996) Processivity of the gene 41 DNA helicase at the bacteriophage T4 DNA replication fork, *J. Biol. Chem. 271*, 16678−16682.
22. Fang, L., Davey, M. J., and O'Donnell, M. (1999) Replisome assembly at oriC, the replication origin of *E. coli*, reveals an explanation for initiation sites outside an origin, *Mol. Cell 4*, 541−553.
23. Funnell, B. E., Baker, T. A., and Kornberg, A. (1987) In vitro assembly of a prepriming complex at the origin of the *Escherichia coli* chromosome, *J. Biol. Chem. 262*, 10327−10334.
24. Kobori, J. A., and Kornberg, A. (1982) The *Escherichia coli* dnaC gene product. II. Purification, physical properties, and role in replication, *J. Biol. Chem. 257*, 13763−13769.
25. Ng, J. Y., and Marians, K. J. (1996) The ordered assembly of the phiX174-type primosome. I. Isolation and identification of intermediate protein-DNA complexes, *J. Biol. Chem. 271*, 15642−15648.
26. Nossal, N. G., Dudas, K. C., and Kreuzer, K. N. (2001) Bacteriophage T4 proteins replicate plasmids with a preformed R loop at the T4 ori(uvsY) replication origin in vitro, *Mol. Cell 7*, 31−41.
27. Frey, M. W., Nossal, N. G., Capson, T. L., and Benkovic, S. J. (1993) Construction and characterization of a bacteriophage T4 DNA polymerase deficient in 3′-5′ exonuclease activity, *Proc. Natl. Acad. Sci. U.S.A. 90*, 2579−2583.
28. Rush, J., Lin, T.-C., Quinones, M., Spicer, E. K., Douglas, I., Williams, K. R., and Konigsberg, W. H. (1989) The 44P subunit of the T4 polymerase accessory protein complex catalyzes ATP hydrolysis, *J. Biol. Chem. 264*, 10943−10953.
29. Nossal, N. G. (1979) DNA replication with bacteriophage T4 proteins. Purification of the proteins encoded by T4 genes 41, 45, 44, and 62 using a complementation assay, *J. Biol. Chem. 254*, 6026−6031.
30. Yang, J., Trakselis, M. A., Roccasecca, R. M., and Benkovic, S. J. (2003) The application of a minicircle substrate in the study of the coordinated T4 DNA replication, *J. Biol. Chem. 278*, 49828−49838.
31. Ishmael, F. T., Alley, S. C., and Benkovic, S. J. (2001) Identification and mapping of protein−protein interactions between gp32 and gp59 by cross-linking, *J. Biol. Chem. 276*, 25236−25242.
32. Valentine, A. M., Ishmael, F. T., Shier, V. K., and Benkovic, S. J. (2001) A zinc ribbon protein in DNA replication: Primer synthesis and macromolecular interactions by the bacteriophage T4 primase, *Biochemistry 40*, 15074−15085.
33. Zhang Z., Spiering, M. M., Trakselis, M. A., Ishmael, F. T., Xi, J., Benkovic, S. J., and Hammes, G. G. (2005) Assembly of the Bacteriophage T4 Primosome: Single Molecule and Ensemble Studies, *Proc. Natl. Acad. Sci. U.S.A. 102*, 3254−3259.
34. Yang, J., Zhuang, Z., Roccasecca, R. M., Trakselis, M. A., and Benkovic, S. J. (2004) The dynamic processivity of the T4 DNA polymerase during replication, *Proc. Natl. Acad. Sci. U.S.A. 101*, 8289−8294.
35. Kadyrov, F. A., and Drake, J. W. (2001) Conditional coupling of leading-strand and lagging-strand DNA synthesis at bacteriophage T4 replication forks, *J. Biol. Chem. 276*, 29559−29566.
36. Liu, C. C., and Alberts, B. M. (1980) Pentaribonucleotides of mixed sequence are synthesized and efficiently prime *de novo* DNA chain starts in the T4 bacteriophage DNA replication system, *Proc. Natl. Acad. Sci. U.S.A. 77*, 5698−5702.
37. Trakselis, M. A., Roccasecca, R. M., Yang, J., Valentine, A. M., and Benkovic, S. J. (2003) Dissociative properties of the proteins within the bacteriophage T4 replisome, *J. Biol. Chem. 278*, 49839−49849.
38. Cha, T.-A., and Alberts, B. M. (1989) The bacteriophage T4 DNA replication. Only DNA helicase is required for leading strand DNA synthesis by the DNA polymerase holoenzyme, *J. Biol. Chem. 264*, 12220−12225.
39. Franklin, M. C., Wang, J., and Steitz, T. A. (2001) Structure of the replicating complex of a pol α family DNA polymerase, *Cell 105*, 657−667.

BI047296W